11-9-2009

Impact of high frequency waves on the ocean altimeter range bias

Douglas C. Vandemark
University of New Hampshire - Main Campus, Doug.Vandemark@unh.edu

Bertrand Chapron
Space Oceanography Laboratory, IFREMER, Plouzané, France

T. Elfouhaily
University of Miami

J. W. Campbell
University of New Hampshire - Main Campus

Recommended Citation

Vandemark, D., B. Chapron, T. Elfouhaily, and J. W. Campbell (2005), Impact of high-frequency waves on the ocean altimeter range bias, J. Geophys. Res., 110, C11006, doi:10.1029/2005JC002979.

Impact of high-frequency waves on the ocean altimeter range bias

D. Vandemark[1]
NASA Goddard Space Flight Center, Wallops Island, Virginia, USA

B. Chapron
Institut Français de Recherche pour l'Exploitation de la Mer (IFREMER)/Centre de Brest, Plouzané, France

T. Elfouhaily[2]
Rosenstiel School of Marine Sciences, University of Miami, Miami, Florida, USA

J. W. Campbell
Ocean Processes Analysis Laboratory, University of New Hampshire, Durham, New Hampshire, USA

Received 28 March 2005; revised 13 June 2005; accepted 12 August 2005; published 9 November 2005.

[1] New aircraft observations are presented on the range determination error in satellite altimetry associated with ocean waves. Laser-based measurements of the cross correlation between the gravity wave slope and elevation are reported for the first time. These observations provide direct access to a long, O(10 m), gravity wave statistic central to nonlinear wave theory prediction of the altimeter sea state bias. Coincident Ka-band radar scattering data are used to estimate an electromagnetic (EM) range bias analogous to that in satellite altimetry. These data, along with ancillary wind and wave slope variance estimates, are used alongside existing theory to evaluate the extent of long- versus short-wave, O(cm), control of the bias. The longer wave bias contribution to the total EM bias is shown to range from 25 to as much as 100%. Moreover, on average the term is linearly related to wind speed and to the gravity wave slope variance, consistent with WNL theory. The EM bias associated with interactions between long and short waves is obtained assuming the effect is additive to the independently observed long-wave factor. This second component is also a substantial contributor, is observed to be quadratic in wind speed or wave slope, and dominates at moderate wind speeds. The behavior is shown to be consistent with EM bias prediction based in hydrodynamic modulation theory. Study implications for improved correction of the on-orbit satellite sea state bias are discussed.

Citation: Vandemark, D., B. Chapron, T. Elfouhaily, and J. W. Campbell (2005), Impact of high-frequency waves on the ocean altimeter range bias, *J. Geophys. Res.*, *110*, C11006, doi:10.1029/2005JC002979.

1. Introduction

[2] The term electromagnetic bias refers to the height difference observed between true mean sea level and that inferred using a radar altimeter. In simplest terms, this EM bias occurs because the reflection of radar signal from wave troughs is greater than from the crests. Field study observations [*Yaplee et al.*, 1971; *Walsh et al.*, 1984; *Arnold et al.*, 1995] and satellite-based work [cf. *Chelton et al.*, 2001] have shown that the bias exists, has a radar frequency dependence and is, to first-order, related to the sea state. To date, the operational satellite correction consists of an empirical algorithm that uses altimeter-derived measurements of sea state and wind speed to estimate this bias for each spacecraft range estimate along its ground track. Still there remains a need to improve this sea level correction as its uncertainty, of O(1%) of significant wave height, now looms large as other terms in the error budget are reduced. Moreover, there is a need to understand when a systematic temporal or spatial error in this correction is occurring [*Kumar et al.*, 2003; *Chelton et al.*, 2001]. Thus a critical remaining need in sea state bias research is to understand when and why the bias varies.

[3] This task has proven difficult to accomplish. The EM bias is associated with nonlinear wave and radar scattering processes that require exacting measurement to resolve and which are seldom recorded. It is also recognized that satellite sensor-specific issues such as the range tracking method, and range corrections as varied as the barotropic, ionospheric, and dual-frequency terms, make direct intercomparison of field, theory, and satellite bias results diffi-

[1] Also with Institut de Recherche sur les Phénomènes Hors Equilibre, CNRS, Marseille, France.

[2] Also at Ocean Process Analysis Laboratory, University of New Hampshire, Durham, New Hampshire USA.

0148-0227/05/2005JC002979

cult. Numerous approaches in theory and field experiments have been used to assess EM bias magnitude and variability through the nondimensional scalar, β, where the absolute bias is written as

$$bias(m) = \beta * H_s, \quad (1)$$

and where H_s is the significant wave height, defined as 4 times the surface elevation standard deviation.

[4] Empirical field studies show a progression from parameterizing β in terms of wind speed and wave height [*Walsh et al.*, 1984, 1991; *Melville et al.*, 1991; *Hevizi et al.*, 1993; *Arnold et al.*, 1995] to the most recent findings that a significant improvement can be gained by parameterization in the RMS slope of longer waves [*Millet et al.*, 2003; *Melville et al.*, 2004]. Thus field observations now suggest that one needs to obtain along-track estimates of the gravity wave slope variance, a variable not readily retrieved from the satellite altimeter.

[5] Theory is divided into several schools. The first shows that a bias can be predicted using weakly nonlinear (WNL) theory [*Longuet-Higgins*, 1963] where three wave interactions among longer gravity waves lead to β estimates of order 2–8% [e.g., *Jackson*, 1979; *Srokosz*, 1986; *Glazman et al.*, 1996; *Gommenginger et al.*, 2003]. The predicted bias is primarily due to a so-called tilt bias or cross-skewness term that arises owing to a nonzero cross correlation between the long-wave elevation and slope. In this case the long waves are nominally considered to be those with wave number less than 10 times that of the wind sea. An extension of this theory includes the geometric or tilt modulation of small $O(1–2$ m) rough ocean surface patches by the underlying wave field [*Rodriguez et al.*, 1992; *Elfouhaily et al.*, 2000]. This model invokes the two-scale hypothesis that short and long waves can be geometrically separated. One result is that the steep centimeter-scale waves act to attenuate WNL predictions made when neglecting their presence. A separate modeling approach [*Rodriguez et al.*, 1992; *Elfouhaily et al.*, 2001] addresses the hypothesis that hydrodynamic modulations, modeled using the conservation of wave action, act to strain centimeter- to meter-scale waves along the phase and elevation of the underlying long waves. This modeled interaction between long and short waves is fundamentally linked to the long-wave orbital velocity and represents a process quite distinct from WNL theory [cf. *Elfouhaily et al.*, 2001; *Chapron et al.*, 2001].

[6] These theories have requisite assumptions and ranges of validity and, not surprisingly, enough uncertainty to preclude comparison beyond order of magnitude with respect to field or on-orbit observations. This is partly because there has been a lack of observational information on the space and time characteristics of the nonlinear sea surface at the wave scales that involve the sea state bias. The resulting lack of constraint can lead to inconsistency in interpretation. For example, *Gommenginger et al.* [2003] exclusively invoke WNL theory to semi-empirically link the EM bias to the wave RMS slope whereas *Melville et al.* [2004] use a ''surrogate'' hydrodynamic modulation theory to do the same. Moreover, the observed radar-frequency dependence of the range bias in past data sets can be predicted using two separate mechanisms [*Rodriguez et al.*, 1992; *Elfouhaily et al.*, 2000, 2001]. One issue that remains open then is the relative importance of the long-wave–driven EM bias versus error driven by interactions between the long and short waves. An answer would help to focus emphasis on the relevant portion of the wave spectrum. For example, is it viable to consider use of ocean wave model spectra and WNL theory in an operational correction application? Or must one also consider that short-wave dynamics, unresolved in both WNL theory and wave spectra modeling, also matter?

[7] As stated above, the ultimate goal of these studies is an improved on-orbit range correction. It has been clear for some time that any new approach must make use of ancillary information to augment the wave height and wind speed (i.e., radar cross section) information from the altimeter. Sources identified for the purpose include scatterometer wind fields, sea surface temperature fields, and global nowcast ocean wave models. Potential benefits of such data are tempered by the fact that their estimates are not available at the equivalent resolution, location, or time of the satellite measurements. How does best use alternate wind and wave data to address improved EM bias correction? One role that field and theoretical EM bias studies can serve is to guide their application. Recent field work [*Millet et al.*, 2003; *Melville et al.*, 2004] makes a compelling case for replacing anemometer wind speed with a gravity wave slope variance estimate in empirical EM bias parameterization. The objective of this paper is to complement those efforts by further deducing the wave scales and processes to highlight. In particular, we focus on this open issue of whether one can solely look to long-wave information in neglect of the role of short centimeter-scale waves.

[8] Several questions can be distilled pertaining to this focus. What is the measured magnitude of the longer wave cross-skewness bias? Is there evidence to support that both this WNL component and long-wave short-wave interactions are involved in the net observed radar range bias? Which wind- and wave-related observations correlate with these bias components and under what conditions? To address these questions we present new aircraft data where long-wave statistics and radar measurements were made in concert. Observations of the EM bias at Ka-band will be reported. We also present cross-skewness observations, derived directly from wave slope and elevation measurements. This is the first time that such tilt bias data have been reported. These quantitative measures provide the opportunity to address the relative importance of the longer wave nonlinear geometry versus hydrodynamic short-wave modulation in sea state bias control. Measurement methods and results follow along with a discussion that includes study implications for satellite correction efforts.

2. Methods

[9] All observations in this study come from an aircraft data collection effort utilizing the National Oceanic and Atmospheric Administration LongEZ research aircraft. The flights took place from 1997 to 1999, mostly in the month of November. Work in 1997 and 1999 was part of the Office of Naval Research Shoaling Waves Experiment while 1998 data come from NASA's Wave Profile Experiment. All data shown herein were collected off the coast of North Carolina

over the mid-Atlantic Bight. The composite data set covers 36 separate flights and more than 2700 individual sea state bias estimates enfolding a spatial ground track of more than 12,000 km. Estimates acquired within 15 km of the coast (depth < 20 m) are omitted to maintain open-ocean conditions. A map of the region and the location of data points can be seen in Figure 3 of *Vandemark et al.* [2004]. The conditions encountered included wind speeds up to 20 m/s and wave heights up to 3.5 m. For more detailed information on the measurement platform and overall experiment details the reader is referred to several recent studies [*Vandemark et al.*, 2001; *Sun et al.*, 2001; *Vandemark et al.*, 2004].

[10] The aircraft measurements that are central to this study are those from a Ka-band scatterometer pointed vertically toward the ocean and three centimeter-precision laser altimeters spaced 0.95 m apart on the airframe and also directed vertically downward to measure the surface elevation at three points surrounding the 1-m-diameter radar footprint [*Vandemark et al.*, 2001, Figure 3]. Specifics of this system and its calibration, motion correction, and data filtering have been described elsewhere [*Vandemark et al.*, 2001; *Sun et al.*, 2001; *Vandemark et al.*, 2004, 1999].

[11] The laser system's three wave elevation estimates are used to infer triply redundant wave elevations (ζ) and wave slopes over 0.95 m spans in orthogonal directions (ζ_x, ζ_y) with respect to the aircraft's heading (along and across the flight track). From these measures it is straightforward to compute parameters relevant to the sea state bias as formulated under weakly nonlinear theory [e.g., *Srokosz*, 1986],

$$bias_{WNL} = -\frac{1}{8}\left(\frac{1}{3}\lambda_0 + \lambda_1\right) H_s, \tag{2}$$

where $\lambda_0 = \dfrac{\langle \zeta^3 \rangle}{\langle \zeta^2 \rangle^{3/2}}$ is the elevation skewness and $\lambda_1 = \dfrac{\langle \zeta \zeta_x^2 \rangle}{\langle \zeta^2 \rangle^{1/2} \langle \zeta_x^2 \rangle} + \dfrac{\langle \zeta \zeta_y^2 \rangle}{\langle \zeta^2 \rangle^{1/2} \langle \zeta_y^2 \rangle}$ is a "cross-skewness" term where here we have neglected the slope-slope terms under the assumption of isotropic wave slope [*Vandemark et al.*, 2004]. The ability to directly measure λ_1 is a primary contribution of this study. This cross correlation between the slope variance and the height is interpreted as being the electromagnetic range bias (or the specular height [*Glazman et al.*, 1996]) that one would observe for a filtered surface having no waves of length scale less than 1–2 m. The direct determination without recourse to a spectral model or theory provides a valuable means to assess the predictions made by many using the WNL formulation of equation (2). The data processing used in this study computes these terms as $bias_{WNL} = \beta_{WNL} H_s = (\beta_s + \beta_t) H_s$ over each 5-km flight segment using roughly 5000 individual slope and elevation measurements. Our computed cross-skewness term, typically seen in the literature as λ_{12}, will be denoted as the tilt bias (β_t) and it should be noted that this bias is associated with the slope variances for waves of length 1–2 m and longer. The skewness bias is denoted as β_s. This term is not strictly associated with the EM bias. The EM bias is the difference between the mean scattering level seen using a radar and true mean sea level while the elevation skewness bias is the height difference between the mean scattering surface and the median [cf. *Chelton et al.*, 2001]. In this paper we will report observed β_s and use it in comparisons with the sea state bias predicted using WNL under equation (2). When EM bias and radar measurements are discussed, they exclude β_s.

[12] The analog to the longer wave slope and elevation cross-correlation (β_t) defines the radar electromagnetic bias where the normalized radar cross section (σ^o) takes the place of the slope variance and the relative bias is then

$$\beta_{Ka} = \frac{\langle \zeta \sigma^o \rangle}{\langle \sigma^o \rangle} H_s^{-1}. \tag{3}$$

[13] A Ka-band radar with radiation wavelength of 0.83 cm was used in this experiment primarily because of the aircraft's small size and low flight altitude. This frequency resides above the typical Ku-band (2.14 cm) satellite altimeter wavelength, but should have a similar value for several reasons. First, the difference in wavelength is small, and though the surface slope and curvature spectra are known to have potentially strong differences at these centimeter scales, one should be able to relate the results at these two frequencies with some confidence. Second, previous results at Ka-band [e.g., *Walsh et al.*, 1984, 1991] suggest the Ka-band bias is significantly lower than that at Ku- or C-band. This result can be assessed here. Finally, future micro-altimeter concepts are in the works using Ka-band designs. EM bias data at Ka-band are thus of great interest in these developments. As with the tilt bias, each β_{Ka} estimate is obtained over a 5-km flight segment.

[14] To make further use of the combined radar, tilt, and skewness bias measurements we can take the additional step of extracting a residual bias under the assumption of a two-scale surface model where the concept divides the surface between nearly linear fast-traveling long waves and short waves, roughly waves with k greater than 10 times the peak spectral wave number. This conceptual model serves several purposes [see *Rodriguez et al.*, 1992; *Elfouhaily et al.*, 2000, 2001; *Chapron et al.*, 2001]. First, it is a prerequisite under hydrodynamic and aerodynamic modulation theories where the shorter waves are modulated along the phase of the longer waves. Second, the scale break is also useful in addressing the typical EM bias field measurements [*Walsh et al.*, 1991; *Arnold et al.*, 1995; *Melville et al.*, 2004] where the radar footprint is of the order of 1 m. In this case, one can independently address the effects of roughness elements within this 1-m facet and the radar scattering from that roughened patch as it tilts owing to linear and nonlinear long-wave effects. Third, *Elfouhaily et al.* [2000] pointed out that weakly nonlinear theory should not be extended down to the short centimeter-scale waves that dominate a radar's σ^o measurement. A break in the spectrum near 1–10 m is one suggestion to avoid violation of the theory's assumptions. The scale break for each of the issues mentioned above are discussed in the noted studies, but the 1- to 2-m separation scale inherent in the present paper's laser and radar observations is reasonably consistent with that suggested for each of these issues.

[15] Two factors discussed in these modeling efforts can be used in the evaluation of our combined sea state bias data. Both *Rodriguez et al.* [1992] and *Elfouhaily et al.* [2000] address the fact that under geometric optics assumption the effective radar, or filtered-surface electromagnetic

bias, will be measurably lower than that predicted under geometrically dictated WNL theory range bias. This arises because the short-wave roughness atop these tilted 1 m facets acts to diffuse the radar scattering which effectively attenuates the nonlinearity in elevation-radar cross-correlation estimate. This is also known as the effect one ignores if one invokes the "horizontal or specular-facet assumption" [e.g., *Jackson*, 1979]. An analytical formulation for this attenuated tilt bias (β_{ta}) is proposed [*Elfouhaily et al.*, 2000] that, to first-order, is given as

$$\beta_{ta} = \lambda_{12}\Delta, \tag{4}$$

where Δ is the ratio of the long-wave (or low frequency) slope variance (mss_l) to the total ($mss = mss_l + mss_s$), $\Delta = \frac{mss_l}{mss_l + mss_s}$, and where mss_s is the short-wave slope variance. This ratio is readily computed using measurements from the field data where the denominator is the total mean square slope for the Ka-band radar, *mss* [see *Vandemark et al.*, 2004]. The scale break imposed between long and short waves is 1–2 m. Therefore β_{ta} pertains to the electromagnetic bias seen under the assumptions of weakly nonlinear theory and geometric optics radar scattering down to a filtered surface of roughly 3 times the radar wavelength, or about 25 mm.

[16] The second modeling component that we make use of is to assume that long-wave short-wave interactions may also play a role in the radar EM bias observations. For example, hydrodynamic modulation can be imposed atop a nonlinear or linear gravity wave field such that a Ka-band radar relative sea state bias can be written as $\beta_{Ka} = \beta_{ta} + \beta_{hydro}$. Two efforts have invoked this process to address β_{hydro} for Ku- and C-band EM bias radar predictions [*Rodriguez et al.*, 1992; *Elfouhaily et al.*, 2001]. Another process proposed in this context is the potential role of wave breaking where an elevation dependence in the short-wave roughness for intermediate-scale waves of order 20–30 cm is predicted [e.g., *Kudryavtsev et al.*, 1999; *Chapron et al.*, 2001].

[17] By combining model-based factors and observed variables, one can compute a residual bias term that removes the WNL component from the total radar EM bias.

$$\beta_{res} = \beta_{Ka} - \beta_{ta}. \tag{5}$$

[18] Variables on the right-hand side are derived from the measurements discussed above. This residual will be examined in the discussion section to explore the agreement between observations and predictions regarding long- and short-wave interactions and the EM bias.

[19] Ancillary data used in this study come primarily from coincident aircraft measurements. These include neutral stability wind speed and friction velocity estimates as well as slope statistics such as the slope variance, skewness, and kurtosis [*Vandemark et al.*, 2004, 2001; *Sun et al.*, 2001]. The slope data at both long and short wavelengths are discussed by *Vandemark et al.* [2004]. In keeping with recent EM bias work that parameterizes the relative bias in terms of RMS slope we derive a slope term, *s*, that accords with the root mean square of the slope variance for a wavelength cutoff of 10 m. This is obtained by scaling our 2-m slope variance, mss_l, by a factor of 0.4 and then taking the square root. The scaling factor was obtained by calibration against wave buoys and wave model spectra [*Gourrion et al.*, 2002]. This 10-m cutoff corresponds both to a typical wave buoy high frequency cutoff ($f_c \sim 0.4$ Hz) and also to the recent EM bias work of *Melville et al.* [2004, Figure 4]. It should be noted that while the slope variance is known to have a nearly 1:1 correspondence with the wind speed, the RMS of this parameter will necessarily differ somewhat. The effect of taking the square root is to alter the probability density function for the observed slopes from a Rayleigh distribution to that of a Gaussian. In essence both high and low slope (wind speed) values are compressed toward the distribution mean. One effect in this case is compression of the dynamic range of the regressor.

[20] One limitation of the aircraft laser altimeter system is inability to cleanly resolve the long-wave directional spectrum without a priori knowledge of wave propagation directions [*Sun et al.*, 2005]. This is mainly a limitation due to aircraft encounter speed with respect to the moving sea surface. One result is our inability to routinely resolve the phase speed of the dominant wave, and hence the wave age or significant slope. Several directional wave measuring buoys were overflown during the course of the data collection, and their spectral output can be used for this purpose in a limited sense.

3. Results

[21] Calculated biases and selected ancillary data are shown for the whole experimental data set in Figure 1. The data sample abscissa for the figure simply represents a discontinuous record of all the flight data over the 36 days. One can see the absolute bias for the radar and cross skewness (tilt bias) track well with each other and with the wind speed, slope variance, and wave height. All variables appear highly correlated. The magnitude of the radar bias exceeds that derived from the laser slope in most cases, but often by only a small percentage. Clearly the tilt bias is a substantial component on its own, suggesting that the longer wave bias is certainly of the order of magnitude of the radar-derived value.

3.1. Long-Wave Range Biases

[22] The relative bias for cross-skewness and skewness terms (β_s and β_t) are shown in Figures 2 and 3. The data have been averaged with the respective regressors. The RMS slope is used in the following presentations to permit evaluations consistent with recent work on the topic [*Gommenginger et al.*, 2003; *Melville et al.*, 2004; *Millet et al.*, 2003].

[23] It is apparent that the skewness bias is small and invariant with the wind. The average observed elevation skewness was 0.09 with a standard deviation of 0.14 and this translates through equation (2) to the levels shown in Figure 2. It is also apparent that β_t is linear with the wind speed for winds above 4 m s^{-1}, and is also linearly increasing with the RMS slope. The sensitivity of the bias to the RMS slope over the range of all data falls below that of the wind speed; one sees a maximum of 3.2% for highest wind and the maximum reached is 2.2% for the highest slope.

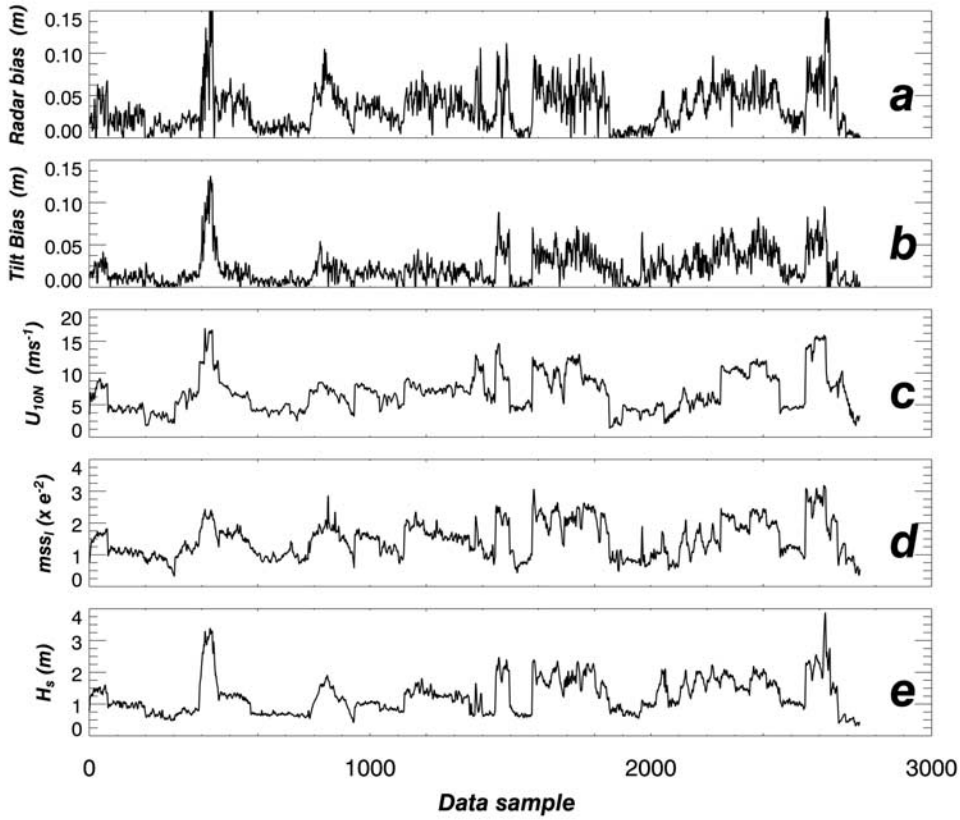

Figure 1. All 5-km-average flight leg samples for the experiment with (a) the radar-derived range bias, (b) the tilt bias, (c) the neutral stability wind speed, (d) the slope variance for waves greater than 2 m, mss_l, and (e) the significant wave height. A three-point boxcar average was applied to each data series.

[24] The linear fit coefficients for β_t shown in Figures 2 and 3 are

$$\beta_t(\%H_s) = 0.51 + 0.15 * U_{10N}\left[for \ * U_{10N} > 4\,\mathrm{ms}^{-1}\right] \quad (6)$$

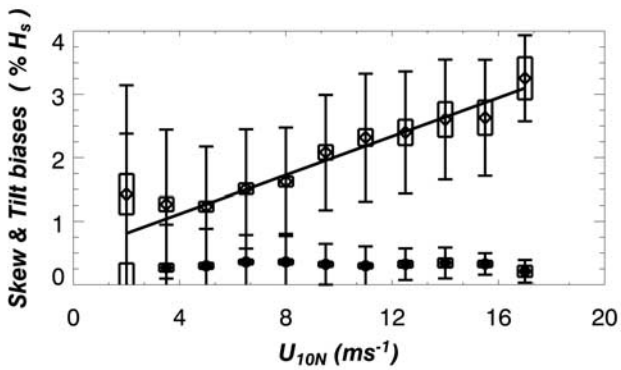

Figure 2. Relative bias measurements versus wind speed. The upper values are the observed relative tilt bias (β_t) for the intermediate scale slopes. The lower symbols represent the elevation skewness term (β_s). Points represent averages over 1.5 m s^{-1} wind speed bins and the whisker plot provides 50% and 95% confidence intervals. The solid curve represents a linear fit through the tilt bias data for wind speeds above 4 m s^{-1}.

and

$$\beta_t(\%H_s) = -0.40 + 26.0 * s. \quad (7)$$

As stated before, these are the first reported measurements of the cross-skewness bias and thus there are no sources for intercomparison.

3.2. Ka-Band EM Bias

[25] The relative bias, β_{Ka}, for the radar is shown in Figures 4 and 5. Similar behavior versus the abscissa is seen

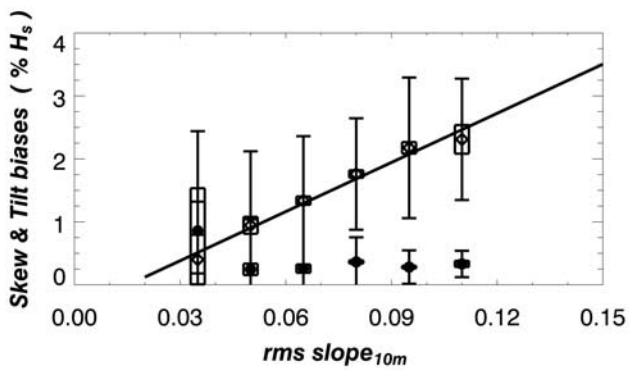

Figure 3. Same as Figure 2 excepting the change of abscissa to the RMS slope for waves greater than 10 m. The solid curve represents a linear fit through the tilt bias data.

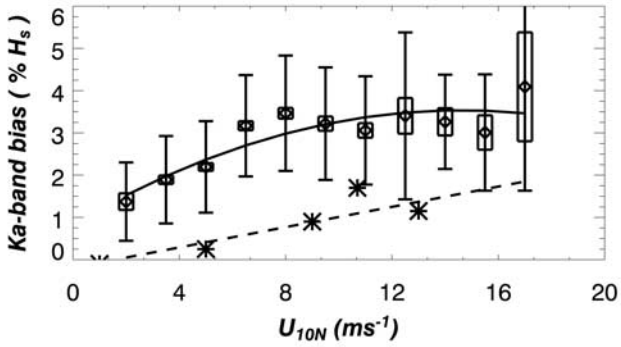

Figure 4. Relative radar bias measurements versus wind speed. The symbols are the observed relative electromagnetic bias (β_t) for a Ka-band radar. Points represent averages over 1.5 m s^{-1} wind speed bins and the whisker plot provides 50% and 95% confidence intervals. The solid curve represents a quadratic fit through the data. The lower curve (dashed line) represents a linear model obtained from the Ka-band data (*) of *Walsh et al.* [1991].

for both the wind and slope regressions. A bias value near 1.0% is seen for the lowest levels, followed by a linear rise up to a near maximum value and then a leveling off or slight decrease with increased wind or slope. This quadratic type of behavior has been seen in previous field studies at Ku- and C-band. In fact, these Ka-band data agree quite well with Ku-band tower results [e.g., *Arnold et al.*, 1995]. The mean level is above 3% for wind speeds exceeding 6 m s^{-1}. Data from *Walsh et al.* [1991] are supplied for comparison and one can see that the present results are of the order of 2% greater than these previous Ka-band measurements. A local maximum is observed in that data as well, but with the limitation of only five data points a linear fit was certainly justified. As noted, the results when compared against the RMS slope of Figure 5 show a similar relationship, and sensitivity across the range of data, to that seen with the wind speed. The data do not tend to zero in either figure. Quadratic fits are applied to both results with limited success as the data do not precisely conform to this assumption. A better description might be a piecewise linear model with a the hinge point at the local maximum that resides at 8 m s^{-1} in wind speed or 0.08 in the RMS slope.

[26] These data were also regressed against the mss_l and friction velocity measurements, and behavior very similar to that seen in Figure 4 is observed. The local maximum for friction velocity was found to occur near 0.23 m s^{-1}.

[27] The quadratic fit coefficients for the curves shown in Figures 4 and 5 are

$$\beta_t(\%H_s) = 0.84 + 0.37 * U_{10N} - 0.013 * U_{10N}^2 \quad (8)$$

and

$$\beta_t(\%H_s) = -0.93 + 73.5 * s - 321.0 * s^2. \quad (9)$$

The observed data scatter for a given wind speed indicates a standard deviation of the order of 2%. Similar deviation magnitudes are seen versus the slope abscissa. The deviations observed here exceed the scatter reported in recently published tower data [*Millet et al.*, 2003; *Melville et al.*, 2004] from the 1990 and 1994 Gulf of Mexico and Bass Straits experiments. Those results represent platform data averaged over a 1-hour time period. Our 5-km spatial data segments, a length dictated by the observed spatial variability in the wave and wind fields, will likely lead to more intrinsic noise in individual bias estimates as 5 km in space translates roughly to 10 min in a temporal estimate. Still, closer examination of the present data set does indicate that some of the observed variability at a fixed wind speed is geophysical.

3.3. An Example of Spatial Complexity

[28] To provide some indication of the variability within this data set we present one example case where the wind-wave conditions can be characterized as being reasonably close to fetch-limited and with a constant wind speed. The aircraft measurements for a single flight leg along the fetch are given. The date was 15 November 1998, and the flight time for this leg ran from 1540 to 1635 UTC. Winds were from the west/southwest at about 8–10 m s^{-1} for the past 12 hours but were weakening at flight time. At the time of the flight the winds were from 290°. Figure 6 shows data as collected from the shore out to more than 200 km to the east on an aircraft heading of 75°. NDBC buoy 44014 was overflown at about 1600 UTC 90 km from shore. At this time the buoy directional wave spectrum showed a wind sea tail at 270°, but a turning sea with the peak energy direction at 240° and a frequency of 0.18 Hz. A weak swell from the NE was also present. Figures 6b and 6c show the wave height, slope variance and friction velocity, u_*. The wind speed, not shown, tracks with u_* and had values of 6.5 to 8 m s^{-1}. Figure 6b shows the wave height and slope increasing with fetch. To gauge how well this case fits with a fetch-limited situation the wave spectrum model of *Elfouhaily et al.* [1997] is used to estimate these parameters based on the measured wind speed and fetch. An offset of 0.3 m in H_s and 0.003 in *mss*, both to adjust for the known swell, were added for all fetches. Wind was adjusted by a factor of 1.1 for all fetches. The modeled results agree well with what is observed. We conclude that a fetch-limited characterization is reasonable. The model's inverse wave age for this case extends from a value of 1.9 nearest shore to about 1.15 at the farthest fetch.

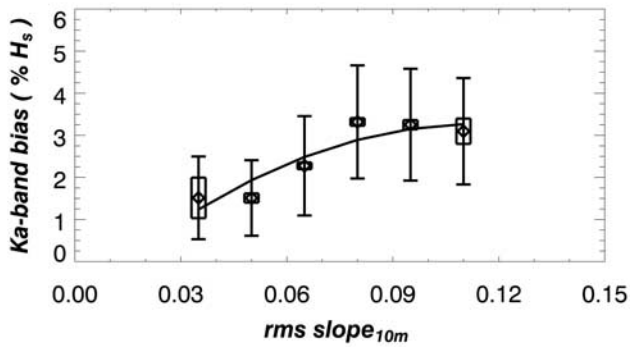

Figure 5. Same as Figure 4 excepting the change of abscissa to the RMS slope for waves greater than 10 m.

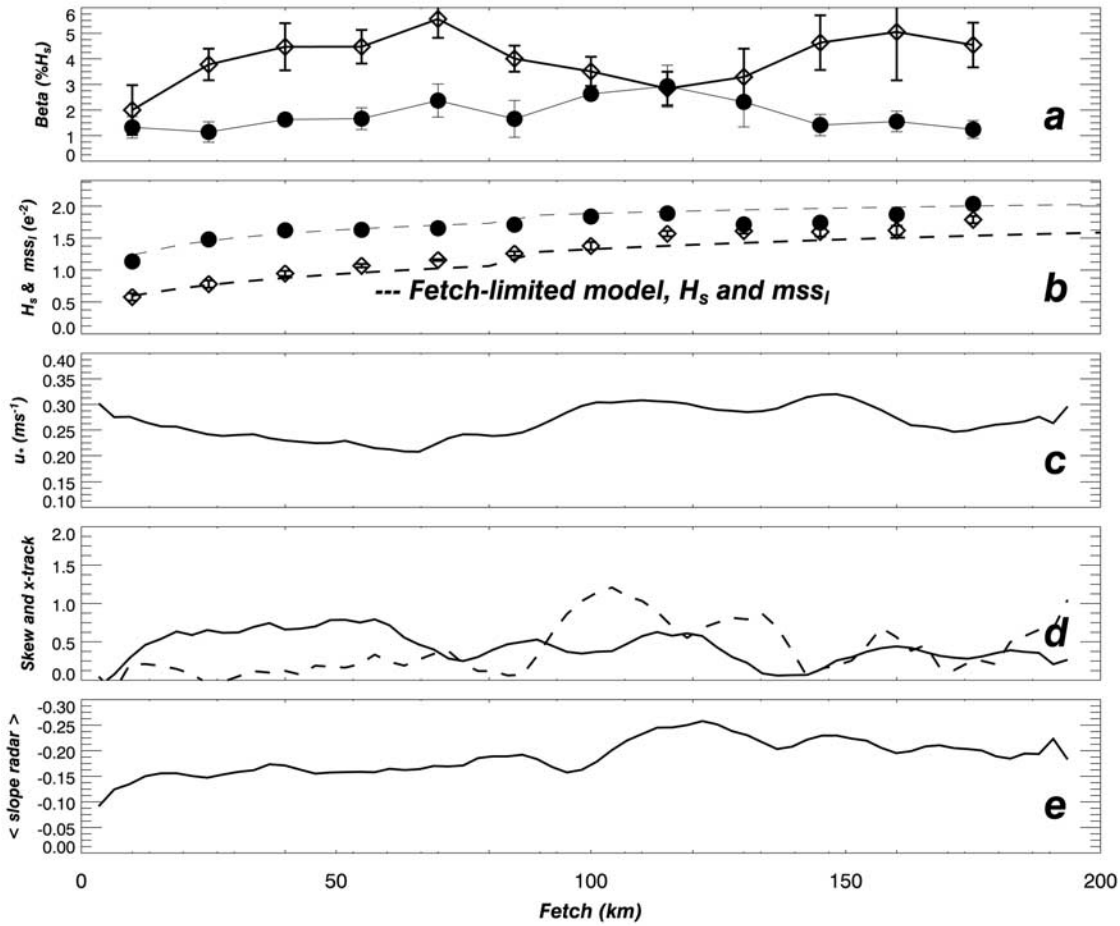

Figure 6. Aircraft measurements versus distance from shore on 15 November 1998. (a) The radar- and laser-derived relative range biases, (b) observed wave height and mean square slope as well as fetch-limited predictions as discussed in text, (c) friction velocity, (d) elevation skewness bias (solid line) and cross-track slope bias (dashed line) as $\%H_s$, and (e) cross correlation between the slope and radar cross section. In each case a 15-km boxcar average has been applied to the data.

[29] The relative radar and tilt biases are shown in the top panel of Figure 6. The larger levels are those for the Ka-band radar. Reference to the previous section shows that the 5.5% magnitude of the bias at a fetch of 50–80 km exceeds the nominal levels seen versus wind or slope values. Moreover, one sees a strong gradient in the radar sea state bias as one heads from shore out to sea. The radar and tilt biases are near each other at the shortest fetch. Then the radar term increases rapidly in the first 20–30 km and then again to a peak at 70 km fetch. However, a significant drop in β_{Ka} occurs after about 70 km and the levels fall to meet β_t at 110 km with a magnitude of 2.8%, nearly half that only 40 km away. The levels then increase as one heads to a fetch of 180 km.

[30] A different result is seen for β_t. This variable has a smaller magnitude and increases more or less linearly with fetch to around 120 km and then decays back to the level nearest shore. A total excursion of about 1.5% is observed.

[31] The ancillary data fields in our aircraft data set were explored for this flight leg to determine if other variables behaved in a similar manner. Figure 6d provides two parameters that may do so. The bias derived from the elevation skewness is the solid curve and it is apparent that the skewness does increase dramatically at short fetch and then continues on to a local maximum near to 50–60 km in fetch. Referring back to our earlier results on the skewness bias, one can see that the bias here exceeds the nominal value (see Figure 2) observed for wind speeds of 6–7 m s^{-1}. In fact, a large value of 0.3 in elevation skewness is observed at 65 km fetch. As shown, the skewness then falls off to lower levels with extended fetch. The other trace on Figure 6d is the tilt bias associated with the cross-track slope (λ_{102}). The value is low up until a fetch of 90 km and then a localized increase is seen for the next 30 to 50 km, one that is inverse to the behavior seen in β_{Ka} in Figure 6a but correlated with a slight increase in β_t in the same panel. Finally, we provide results from a diagnostic variable that is carried in the data set. The lowest panel provides the cross correlation between the individual slope modulus (ζ_{2D}) and σ^o. This average value of this term for the multiyear data set is -0.14 and the largest level is -0.36. Physically, this correlation is expected and would be -1.0 if there were only longer waves on the surface controlling all radar return power. What is seen in Figure 6e is that this correlation increases significantly near a fetch of 100 km, perhaps in tandem with the cross-track tilt term in Figure 6d. The local

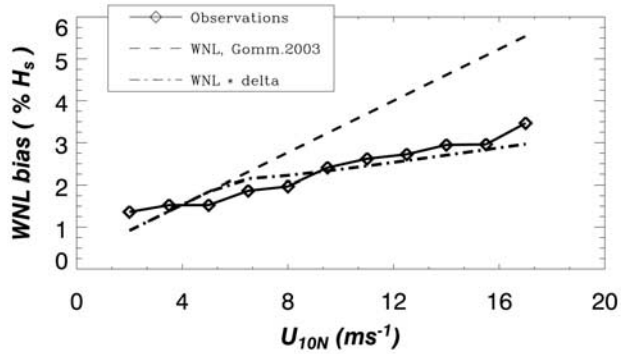

Figure 7. Upper curve is the tilt + skewness bias (β_{WNL}) prediction from a two-dimensional realization of weakly nonlinear theory where the high-frequency cutoff is taken to be 10 k_p. The bottom trace is WNL theory for a 2-m wavelength cutoff using the factor Δ as discussed in the text. Observations are the bin-averaged result combining the skewness and cross-skewness terms of equation (2).

increase indicates increased reflection of the tilted facet field in the radar cross-section data. Thus data in Figures 6d and 6e indicate a localized increase in the longer-wave tilt that may effectively reduce the radar EM bias near this fetch.

4. Discussion

[32] A new contribution from this study is the direct measurement of range biases associated with wavelengths longer than 1–2 m. That is, the laser-derived results of β_t provide a measure of the EM bias that is mostly devoid of the gravity-capillary waves that contribute greatly to the complexity in modeling and predicting the radar EM bias. The results presented show that a linear behavior versus wind speed and the RMS slope emerges. To compare this with theoretical predictions the skewness and cross-skewness data are combined to compute β_{WNL} and averaged versus wind speed as shown in Figure 7. We find that at all but light winds the observation falls significantly below numerous previous model studies [e.g., *Jackson*, 1979; *Srokosz*, 1986; *Rodriguez et al.*, 1992; *Glazman et al.*, 1996] involving weakly nonlinear theory. That conclusion is illustrated in Figure 7 where the two-dimensional WNL theory prediction is given along with the observation-based result. The theoretical long-wave result is for that portion of the wave number spectrum integrated out to 10 times the peak wave number. As shown by *Gommenginger et al.* [2003] and elsewhere, extension of this theory to include shorter waves (higher wave numbers) does not substantially lower this prediction. It is seen that the magnitude of the model is a factor of 1.5–1.9 above the data. However, it is encouraging that the observations and model both show a linearly increase with wind speed. This is also found to be the case for the model and data intercomparisons versus the long-wave RMS slope and slope variance (not shown).

[33] Moreover, if one attenuates the WNL prediction in the manner described in equation (4) and by *Elfouhaily et al.* [2000], then one finds that model and observation draw close in magnitude as well. In this instance, the wavelength separation scale for the slope variance ratio term Δ would be 10 k_p while the denominator, the total variance, would be our measured 2-m slope variance term mss_t. This ratio can be approximated by following *Phillips* [1977] to derive mss_{10kp} for a fully developed wind sea given the wind speed [see also *Vandemark et al.*, 2004]. We find $\Delta(k_p)$ will extend from a value of 1.0 for winds up to 5 m s^{-1} and then quickly decay to a value near 0.5 for wind speeds above the low wind regime. While this is admittedly a first-order estimate lacking the true k_p, application of this Δ factor in Figure 7 aligns the theory and observations to within 10–20% for moderate to high wind speeds. We suggest that this is a fairly remarkable confirmation of the tilt bias predicted using composite scale WNL theory for wavelengths greater than 1–2 m.

[34] Thus one now has some quantifiable validation of the most pertinent model for the electromagnetic bias associated with the longer waves, both in terms of the magnitude and dependence on the wind speed. The present data must be considered as representing only a limited range of wave conditions (see Figure 1), but a range that model predictions are able to encompass.

[35] Moreover, the results cement the knowledge that cross skewness is, to first-order, linear in short-wave roughness and/or wind speed, as well as in the longer wave slope variance. This variable does not show the quadratic behavior, often attributed to long-wave short-wave modulations, that is seen in the radar EM bias data at C-, Ku- and now Ka-band. *Elfouhaily et al.* [2000] postulated that the intermediate-scale waves, λ of $O(1-10$ m), may be subject to such nonlinear wave hydrodynamics. The present data on β_t suggest that if it is present, the impact of the effect on the tilt bias certainly differs from that observed versus wind speed within the radar EM bias at any frequency reported to date in field and on-orbit studies.

[36] The EM bias field observation literature is limited to only a handful of measurement programs. Figures 4 and 8 suggest that the present Ka-band aircraft data agree more closely with tower observations at Ku-band than with the 160-m-height aircraft observations at Ka-band reported by *Walsh et al.* [1991]. That earlier airborne program also reported C- and Ku-band results at 160 m height (*Hevizi et al.* [1993] that fall somewhat below tower measurement results at C- and Ku-band [*Melville et al.*, 1991; *Arnold et al.*, 1995; *Melville et al.*, 2004]. The aircraft sensors, data collection, and analysis techniques of *Walsh et al.* [1991]

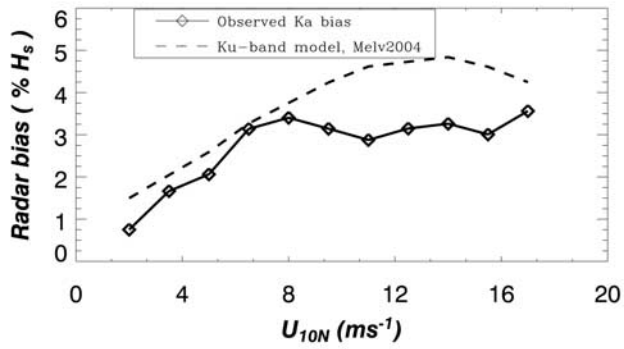

Figure 8. Ka-band bias results as seen in Figure 4 and experiment-derived Ku-band model results using equation (16) of *Melville et al.* [2004].

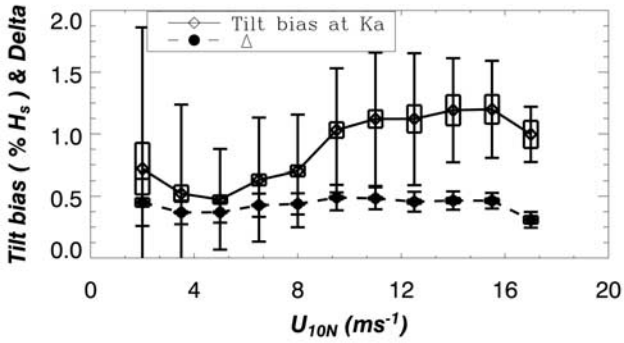

Figure 9. Cross-skewness bias (β_{ta} as computed for a Ka-band altimeter as derived from λ_1 and Δ observation using equation (4). The separation scale for long and short waves in Δ is 2 m, and the short-wave slope variance is derived using the Ka-band backscatter as discussed in the text. Resulting attenuation in β_t can be observed through comparison to Figure 2.

and *Hevizi et al.* [1993] differ substantially from those used in the LongEZ measurements collected for this study for which the altitudes (10–25 m) and equipment are much more closely aligned to the tower measurement programs. However, these studies [*Walsh et al.*, 1991; *Hevizi et al.*, 1993] computed EM bias as the range difference between the computed centroid of the radar power weighted elevations and the centroid of the elevation data alone. This is equivalent to equation (3). The measurement discrepancy has been cited before, and we do not have information to clarify the difference.

[37] Overall, the comparison of Ku- and Ka-band results shown in Figure 8 suggests that the Ka value lies only slightly below the Ku-band up to winds near 8 m s^{-1} and then flattens off to a value that lies 1 to 1.5% of β below the Ku-band level. The bin-averaged realization of the Ku-band model is built using the cubic equation (16) of *Melville et al.* [2004] and our field observations of the wind speed and wave height as input. Thus the joint wind and wave height conditions for the two experiments should be equalized somewhat in Figure 8. Therefore present data suggest that while Ka-band data do fall below the Ku-band results, they do so by less of a factor than previously reported [*Walsh et al.*, 1991] and the frequency difference is most apparent at the higher wind speeds. We note that the comparison when done in terms of the RMS slope and equation (18) of *Melville et al.* [2004], though not shown, yields results similar to Figure 8.

[38] Figures 9 and 10 provide results at Ka-band for β_{ta} and Δ and the subsequent residual EM bias derived using our observations and equations (4) and (5). As in Figure 7, one sees an attenuation of the cross skewness in Figure 9. Δ is only a weak function of wind speed and varies little from its mean value near 0.4. Note that this term β_{ta} will increase with decreasing radar frequency such that Ku- and C-band sensors would carry higher tilt biases within their EM bias [*Elfouhaily et al.*, 2000].

[39] The error bars for β_{res} in Figure 10 show significant scatter but the mean results suggest a strong rise with wind speed from near zero at low winds to a maximum value of 2.3% near a wind speed of 8 m s^{-1}. The value then falls off to a value near 1.5% as winds become moderate to strong. The relative EM bias contributions of the longer wave tilt bias and this residual are seen in these two figures. At light and strong winds both components are nearly of the same order while for moderate wind speeds the residual component exceeds the tilt term by as much a factor of 3. The residual derivation was also carried out versus RMS slope and we find similar results where removal of the tilt bias leaves a nonlinear residual behavior versus the abscissas and relative contributions vary versus the RMS slope similarly to that with increasing wind.

[40] The agreement between observed β_{res} and the first-order hydrodynamic theory prediction at Ku-band [*Elfouhaily et al.*, 2001] is remarkable. The results are also in qualitative agreement with the hydrodynamic model prediction seen in Figure 9 of *Rodriguez et al.* [1992] where the deep phase (i.e., quasi-optical) approximation is suggested to be applicable for comparison to results from a Ka-band system. Both theory and observations suggest a local maximum in wind speed and subsequent fall-off as winds become strong. While this behavior has several possible physical interpretations, the close agreement with the well-known hydrodynamic modulation theory suggests that this observational product β_{res} provides some validation of that approach. Most apparent, however, are the facts that this residual component is not negligible, is associated with wavelengths less than 2 m, and is not linearly related to wind speed or the longer wave slope variance. The last observation points to an observed difference between WNL and residual components.

[41] Most of the discussion and data presentation here is focused upon mean relationships between bias terms and wind and wave statistics. The fetch-limited case of Figure 6 is presented to provide some view of variability within the data. This case where wind speed is nearly constant is provided as evidence that the observed tilt and radar bias observations are: (1) not simply related to either the wind speed or the longer wave slope variance and (2) that the standard deviations seen in the error bars of Figures 2 through 5 are associated at least in part with geophysical

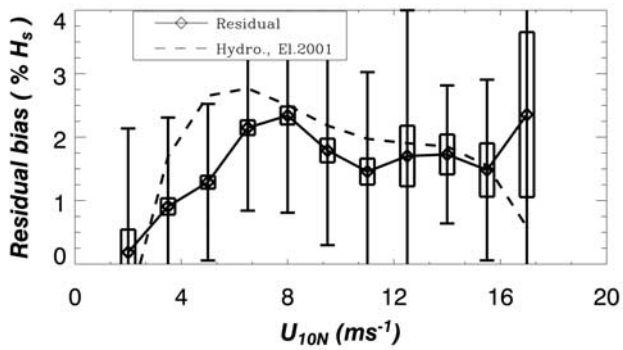

Figure 10. The residual EM bias at Ka-band as derived using equation (5) along with the laser and radar-derived range biases and slope variance data. Both the 50 and 95% confidence intervals are shown for the bin-averaged result. The model curve is the hydrodynamic theory EM bias for wind and wave aligned conditions at Ku-band as seen by *Elfouhaily et al.* [2001].

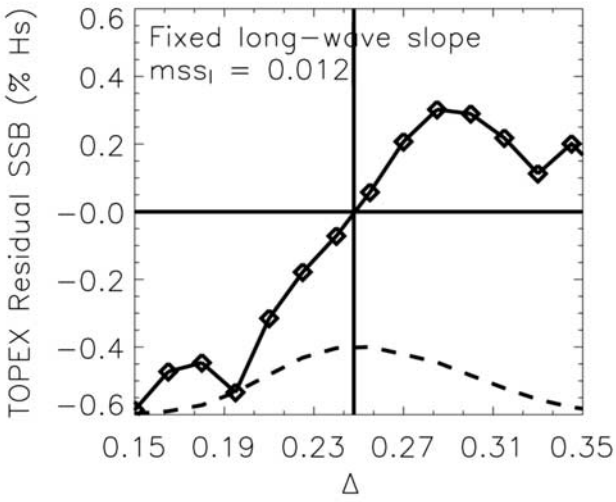

Figure 11. Residual sea state bias at Ku-band versus Δ as derived from the TOPEX altimeter using averaging of the sea level anomaly data for a constant long-wave mean square slope of 0.012 ± 0.001. The curve at bottom represents the normalized probability density of derived Δ (see text for Δ retrieval information). Total sample population is 155,605. The mean sea state bias for this case is 2.9%.

variability not encompassed by any univariate relationship. The conditions dictating the range bias for Figure 6 appear to be somewhat complex. One hypothesis is that a turning and likely multimodal wave spectrum after 80 km in fetch breaks down a large radar EM bias that is associated with strongly directional and growing long wind wave field. The initial rise with fetch coincides with a high elevation skewness, and hence strong directionality and likelihood of a steepened sea. The observed large β_{Ka} at short fetch is then associated with some form of short-wave modulation with respect to the wave elevation, whereas the laser-derived tilt bias shows no such extreme behavior. That is, differences between the tilt bias and the radar suggest that no simple WNL theory explanation will suffice here. The decrease in the radar bias and slight increase in the tilt bias from 80 to 130 km appear to be associated with a change in the overall wave field directionality as suggested by Figures 6d and 6e. The slight increase in the friction velocity at this fetch may also support the notion of a change in the wave field. One important discussion point for this case is that the radar data do not strongly correlate with wind speed or RMS slope. However, both the tilt and radar bias terms do follow the slope better than they do the wind speed.

[42] This study does not deal explicitly with EM bias parameterization, nor do the data indicate a clear difference between EM bias correlation with wind speed and with RMS slope that has been reported elsewhere [*Millet et al.*, 2003; *Melville et al.*, 2004]. In those efforts the same Ku-band tower data are used to show that use of H_s and s improves upon the traditional model formed using H_s and U_{10N}. The present study certainly affirms that relationships in s can be found for both β_{ta} and β_{res}, our observed components making up the total Ka-band EM bias. Moreover, the overall quadratic nature of the tower Ku-band results shown in Figure 8 hint that a β_{res} term derived at Ku-band would yield a result similar to that of Figure 10. Thus the Ku-band tower results appear to be reasonably consistent with the Ka-band results shown in the present study in the overall sense of tilt and long-short wave bias contributions.

[43] Regarding implications for improved satellite sea state bias corrections, this study strongly supports theoretical claims that both long-wave nonlinearities and long-short wave interactions contribute to the EM bias. One key ramification is that both long and short wavelengths and their covariance need to be considered in any empirical correction solutions.

[44] Numerous recent papers highlight the dominance of the EM bias by the RMS slope which in turn has been shown to correspond to the bias predicted under WNL theory and, to some extent, under long-wave short-wave interaction theory. A stated implication [*Gommenginger et al.*, 2003; *Kumar et al.*, 2003; *Melville et al.*, 2004] is that a long-wave focus is likely to be sufficient for on-orbit corrections. However, this study finds that the two-scale WNL theory appears to be relevant with the corresponding implication that both the long-wave field cross-skewness bias predictor and its attenuation by shorter waves matter. The WNL scaling factor $\Delta \approx \frac{mss_l}{mss}$ of equation (4) is thus a possible EM bias perturbation term and therefore $mss \propto \sigma^{o-1}$, a term dominated by short waves, can become important.

[45] To test this hypothesis of short-wave relevance, we call upon on-orbit data created for empirical SSB correction studies. The long-wave slope data for this exercise are derived from a global ocean wave model and then colocated with the altimeter measurements. This satellite/wave model data set (H. Feng et al., Assessment of wind field impacts on wave model output the TOPEX altimeter, submitted to *Journal of Ocean Engineering*, 2005) is the foundation for future study and its description and application lie outside this paper's scope. The point here will be to assess just one satellite implication of the present study. Figure 11 shows the magnitude of the computed residual relative sea state bias obtained from TOPEX satellite height anomaly data [*Vandemark et al.*, 2002] under the condition where the long-wave mean square slope value is held constant. The abscissa is the scaling term of 4, where the numerator is the fixed long-wave value ($mss_l = 0.012$) and the denominator is retrieved using the satellite σ^o at Ku-band, Geometrical-Optics theory and a Fresnel factor of 0.45 [e.g., *Vandemark et al.*, 2004]. While a solely slope-driven EM bias would be constant in Figure 11, one sees the residual adjust with the scaling factor as predicted by two-scale theory. That is, as the total slope variance increases (decreases) the EM bias decreases (increases). The total range of bias residual associated with σ^o dynamics is about 1% of H_s, a range that is significant in satellite correction efforts. We conclude that while the long-wave emphasis is certainly important, both this study's field data and these satellite-based results indicate a multivariate approach must include shorter-wave information such as the radar cross-section data. A similar consistency with two-scale WNL theory has been seen in deriving on-orbit C- and K-band sea state bias models (S. Lebroue, personal communication, 2005) and comparing

their differences (through Δ) with the radar backscatter retrieved at C- and Ku-band using the Jason-1 satellite.

5. Conclusions

[46] Field studies of the EM bias permit lines of inquiry that are unavailable from the satellite perspective. Observations reported here, particularly the new cross-skewness information, provide a first direct validation of theoretical prediction using weakly nonlinear gravity wave theory. The magnitudes observed suggest that this long-wave nonlinearity is only partially responsible for the observed radar EM bias. Together, the radar and cross-skewness data are shown to behave consistently with a conceptual EM bias model where two processes, the long-wave tilt bias and the interaction of short and long waves, coexist and are of the same order. In both cases it is suggested that the interplay between slope variances associated with centimeter-scale waves and longer waves will serve as a perturbation factor in observed sea state bias levels.

[47] Ultimately, such findings must apply to on-orbit satellite range correction improvements. The present study indicates several important points in this respect. Foremost is the fact that short centimeter-to-meter scale wavelengths must be considered in satellite inversions. This is inconsistent with recent suggestions that long-wave slope information, perhaps derived from a global model for the long-wave directional spectrum, might be solely sufficient for satellite EM bias improvement. One explicit satellite-based example of this multivariate or multiscale nature of the EM bias is given in the discussion section above (Figure 11). This re-emphasizes the need for short-wave observation surrogates in on-orbit studies possibly including the altimeter radar cross section (C- and Ku-band) and derived winds, scatterometer cross section and winds, and reanalysis model wind fields. Another point to take from this study is that utilization of two-scale WNL predictions [*Elfouhaily et al.*, 2000] may indeed serve quantitative on-orbit work. This falls very much in line with recent studies predicting the bias through the long-wave RMS slope [e.g., *Gommenginger et al.*, 2003], but with the inclusion of the short-wave influenced Δ factor such that this WNL component is only a partial but important contributor. Finally, the observed quadratic dependence for the radar bias in either wind speed or RMS slope differs substantially from the linear behavior observed here and predicted elsewhere under weakly nonlinear long-wave theory for the cross-skewness term. The clear differences between observed λ_{12}, measured at 2-m-length scale, and the radar bias carrying waves down to 1–2 cm again suggest that parameterizing the processes occurring at the wavelengths between these two limits is important to ongoing correction improvement efforts.

[48] **Acknowledgments.** Thanks to D. Hines, E. Dumas, G. Crescenti, J. French, J. Sun, S. Burns, D. Vickers, and L. Mahrt for their work in the sensor design, operation, data collection and processing, and most of all to Timothy Crawford, the essential element in all of this work, and a scientist who is greatly missed. This work was funded by NASA's Science Directorate and by Office of Naval Research grant N0001497-F-0179.

References

Arnold, D. V., W. K. Melville, R. H. Stewart, J. A. Kong, W. C. Keller, and E. Lamarre (1995), Measurements of electromagnetic bias at Ku-bands and C-bands, *J. Geophys. Res.*, *100*(C1), 969–980.

Chapron, B., D. Vandemark, T. Elfouhaily, D. R. Thompson, P. Gaspar, and S. LaBroue (2001), Altimeter sea state bias: A new look at global range error estimates, *Geophys. Res. Lett.*, *28*(20), 3947–3950.

Chelton, D. B., J. Ries, B. Haines, L.-L. Fu, and P. Callahan (2001), Satellite altimetry, in *Satellite Altimetry and Earth Sciences—A Handbook of Techniques and Applications*, edited by L.-L. Fu and A. Cazenave, pp. 1–132, Elsevier, New York.

Elfouhaily, T., B. Chapron, K. Katsaros, and D. Vandemark (1997), A unified directional spectrum for long and short wind-driven waves, *J. Geophys. Res.*, *102*(C7), 15,781–15,796.

Elfouhaily, T., D. R. Thompson, B. Chapron, and D. Vandemark (2000), Improved electromagnetic bias theory, *J. Geophys. Res.*, *105*(C1), 1299–1310.

Elfouhaily, T., D. R. Thompson, B. Chapron, and D. Vandemark (2001), Improved electromagnetic bias theory: Inclusion of hydrodynamic modulations, *J. Geophys. Res.*, *106*(C3), 4655–4664.

Glazman, R., A. Fabrikant, and M. A. Srokosz (1996), Numerical analysis of the sea state bias for satellite altimetry, *J. Geophys. Res.*, *101*(C2), 3789–3799.

Gommenginger, C. P., M. A. Srokosz, J. Wolf, and P. Janssen (2003), An investigation of altimeter sea state bias theories, *J. Geophys. Res.*, *108*(C1), 3011, doi:10.1029/2001JC001174.

Gourrion, J., D. Vandemark, S. Bailey, and B. Chapron (2002), Investigation of C-band altimeter cross section dependence on wind speed and sea state, *Can. J. Remote Sens.*, *28*(3), 484–489.

Hevizi, L. G., E. J. Walsh, R. E. McIntosh, D. Vandemark, D. E. Hines, R. N. Swift, and J. F. Scott (1993), Electromagnetic bias in sea-surface range measurements at frequencies of the TOPEX/Poseidon satellite, *IEEE Trans. Geosci. Remote Sens.*, *31*(2), 376–388.

Jackson, F. (1979), The reflection of impulses from a nonlinear random sea, *J. Geophys. Res.*, *84*(C8), 4939–4943.

Kudryavtsev, V. N., V. K. Makin, and B. Chapron (1999), Coupled sea surface-atmosphere model: 2. Spectrum of short wind waves, *J. Geophys. Res.*, *104*(C4), 7625–7639.

Kumar, R., D. Stammer, W. K. Melville, and P. Janssen (2003), Electromagnetic bias estimates based on TOPEX, buoy and wave model data, *J. Geophys. Res.*, *108*(C11), 3351, doi:10.1029/2002JC001525.

Longuet-Higgins, M. S. (1963), The effect of non-linearities on statistical distributions in the theory of sea waves, *J. Fluid Mech.*, *17*(3), 459–480.

Melville, W. K., R. H. Stewart, W. C. Keller, J. A. Kong, D. V. Arnold, A. T. Jessup, M. R. Loewen, and A. M. Slinn (1991), Measurements of electromagnetic bias in radar altimetry, *J. Geophys. Res.*, *96*(C3), 4915–4924.

Melville, W. K., F. C. Felizardo, and P. Matusov (2004), Wave slope and wave age effects in measurements of electromagnetic bias, *J. Geophys. Res.*, *109*, C07018, doi:10.1029/2002JC001708.

Millet, F. W., D. V. Arnold, K. F. Warnick, and J. Smith (2003), Electromagnetic bias estimation using in situ and satellite data: 1. RMS wave slope, *J. Geophys. Res.*, *108*(C2), 3040, doi:10.1029/2001JC001095.

Phillips, O. M. (1977), *The Dynamics of the Upper Ocean*, 2nd ed., Cambridge Univ. Press, New York.

Rodriguez, E., Y. J. Kim, and J. M. Martin (1992), The effect of small-wave modulation on the electromagnetic bias, *J. Geophys. Res.*, *97*(C2), 2379–2389.

Srokosz, M. A. (1986), On the joint distribution of surface elevation and slopes for a nonlinear random sea, with an application to radar altimetry, *J. Geophys. Res.*, *91*(C1), 995–1006.

Sun, J. L., D. Vandemark, L. Mahrt, D. Vickers, T. Crawford, and C. Vogel (2001), Momentum transfer over the coastal zone, *J. Geophys. Res.*, *106*(D12), 12,437–12,448.

Sun, J. L., S. P. Burns, D. Vandemark, M. A. Donelan, L. Mahrt, G. Crescenti, J. French, and T. Herbers (2005), Measurement of directional wave spectra using aircraft laser altimeters, *J. Atmos. Oceanic Technol.*, *22*(7), 569–885.

Vandemark, D., T. Crawford, R. Dobosy, T. Elfouhaily, and B. Chapron (1999), Sea surface slope statistics from a low-altitude aircraft, paper presented at International Geoscience and Remote Sensing Symposium, Inst. of Electr. and Electron. Eng., Hamburg, Germany.

Vandemark, D., P. D. Mourad, S. A. Bailey, T. L. Crawford, C. A. Vogel, J. Sun, and B. Chapron (2001), Measured changes in ocean surface roughness due to atmospheric boundary layer rolls, *J. Geophys. Res.*, *106*(C3), 4639–4654.

Vandemark, D., N. Tran, B. Chapron, B. D. Beckley, and P. Gaspar (2002), Direct estimation of sea state impacts on radar altimeter sea level estimates, *Geophys. Res. Lett.*, *29*(24), 2148, doi:10.1029/2002GL015776.

Vandemark, D., B. Chapron, J. Sun, G. H. Crescenti, and H. C. Graber (2004), Ocean wave slope observations using radar backscatter and laser altimeters, *J. Phys. Oceanogr.*, *34*, 2825–2842.

Walsh, E. J., D. W. Hancock, D. E. Hines, and J. E. Kenney (1984), Electromagnetic bias of 36-GHz radar altimeter measurements of MSL, *Mar. Geod.*, *8*(1–4), 265–296.

Walsh, E. J., et al. (1991), Frequency dependence of electromagnetic bias in radar altimeter sea surface range measurements, *J. Geophys. Res.*, *96*(C11), 20,571–20,583.

Yaplee, B., A. Shapiro, D. Hammond, and E. Uliana (1971), Nanosecond radar observations of the ocean surface from a stable platform, *IEEE Trans. Geosci. Eng.*, *9*, 170–174.

J. W. Campbell, Ocean Processes Analysis Laboratory, University of New Hampshire, Morse Hall, Room 142, Durham, NH 03824, USA. (janet.campbell@unh.edu)

B. Chapron, Institut Français de Recherche pour l'Exploitation de la Mer (IFREMER)/Centre de Brest, DRO/OS, BP70, F-29280 Plouzané, France. (bertrand.chapron@ifremer.fr)

T. Elfouhaily, Rosenstiel School of Marine and Atmospheric Science, University of Miami, 4600 Rickenbacker Causeway, Miami, FL 33149, USA. (telfouhaily@rsmas.miami.edu)

D. Vandemark, NASA/GSFC, Biospheric and Hydrospheric Laboratory, Building N-159, Wallops Island, VA 23337, USA. (douglas.vandemark@nasa.gov)